

Investigation of Plastic Hinge Length of Reinforced Concrete Wall

Doaa Talib Hashim¹, Alyaa A. Al-Attar², Nabeel A. H. Kzar³
doaatlib7@gmail.com¹, dr.alayaa@ntu.edu.iq², engineerabee19@gmail.com³

Mustansiriyah University, Baghdad, Iraq¹, Northern Technical University, Mosul, Iraq², Holy Karbala Municipalities, Hindiya Municipality, Karbala, Iraq³

Abstract. This study investigates the effect of certain parameters on the magnitude of plastic hinge length of RC shear walls and proposes an analytical expression for estimating the plastic hinge length. A finite element model was analyzed and validated with experimental test results for an existing study and a parametric study was performed for it. The established results were according to several parameters such as axial load ratio, slenderness ratio and wall length. The numerical results showed a different impact of these parameters on the formation of the plastic hinge length. In this study, a new simple expression was derived based on those parameters using statistical package software. Proposed plastic hinge expression was compared with the results of the plastic hinge length obtained from FE analysis. Finally, the accuracy of the proposed equation was validated by using the shear wall results from the literature researches.

Keywords: Plastic hinge length, Reinforced shear wall, Parametric study, Finite Element Analysis.

1 Introduction

The determination of the amount and location of plastic deformations in RC shear wall considered a significant step for describing the performance of the shear wall building system in seismic loading. Many researchers have developed empirical models to investigate the parameters that affect the magnitude of the plastic hinge region and to derive equations to calculate the length of the plastic hinge in reinforced concrete elements depending on test results. The plastic hinge method and the derived analysis are still used widely in displacement-based seismic design and performance evaluation procedures for estimating the inelastic displacement demand and capacity [1]. The plastic curvature can be calculated by the total curvature as shown in equation (1). By integrating the inelastic curvature, the inelastic rotation was as shown in equation (2). Besides, by integrating the inelastic rotation, the inelastic displacement after considering the net height is shown in equation (3).

$$\phi_p = \phi - \phi_y \quad (1)$$

$$\theta_p = \phi_p L_p \quad (2)$$

$$L_n = L - \frac{L_p}{2} \quad (3)$$

$$\Delta_p = \theta_p L_n \quad (4)$$

$$\Delta_p = (\phi - \phi_y) L_p \left[L - \frac{L_p}{2} \right] \quad (5)$$

After combine equations 1 and 5 the total displacement is shown in equation (6). By integrating the elastic curvature, the yield displacement can be established. It was assumed that the elastic curvature linear (equation 7). As a result, the total displacement is shown in equation (8).

$$\Delta_f = \Delta_y + \Delta_p = \Delta_y + (\phi - \phi_y) L_p \left[L - \frac{L_p}{2} \right] \quad (6)$$

$$\Delta_y = \frac{\phi_y L^2}{3} \quad (7)$$

$$\Delta = \frac{\phi_y L^2}{3} + (\phi - \phi_y) L_p \left[L - \frac{L_p}{2} \right] \quad (8)$$

The shear deformation in slender concrete walls was estimated using the developed experiential equation [2]. This experiential equation was formulated based on a series of experimental and analytical studies of slender RC walls under seismic loading as shown in the following equations (9) and (10).

$$\Delta_{sh} = 1.5 \Delta_f \left[\frac{\epsilon_m}{\phi \tan \beta} \right] \frac{1}{h_w} \quad (9)$$

$$\Delta_u = \Delta_f + \Delta_{sp} + \Delta_{sh} = \left(\frac{1}{3} \phi_e h_w^2 + \frac{2}{3} \phi_e L_{sp} h_w + \phi_p L_p h_w \right) \left(1 + 1.5 \left(\frac{\epsilon_m}{\phi \tan \beta} \right) \frac{1}{h_w} \right) \quad (10)$$

Besides, an expression has been proposed to calculate the plastic hinge length in Eurocode 8 as shown in equation (11). Where: L_v = shear span (moment-shear ratio, M/V), d_{bl} = (mean) diameter of the tension reinforcement [3].

$$L_p = \frac{L_v}{30} + 0.2 L_w + \frac{d_{bl} f_y (MPa)}{\sqrt{f'_c (MPa)}} \quad (11)$$

In addition, tests have been conducted on reinforced concrete members by applying uniaxial bending load, with and without axial loads in order to derive expressions for plastic hinge length and deformations at yielding, according to the member geometric and mechanical properties [4]. They developed equations (12) and (13) to calculate the length of plastic hinge for cyclic loading and monotonic loading, respectively.

$$L_{p,cy} = 0.12 L_s + 0.014 \alpha_{sl} f_y d_b \quad (12)$$

$$L_{p,mon} = 1.5 L_{p,cy} = 0.18 L_s + 0.021 \alpha_{sl} f_y d_b \quad (13)$$

A finite element analysis model has been conducted and validated by test results on RC structural wall [5]. They proposed an expression depending on the results of nonlinear finite element analysis for L_p as a function of wall length, moment-shear ratio, and axial compression equation (14).

$$L_p = (0.2L_w + 0.05L_v)\left(1 - 1.5\frac{P}{A_w f'_c}\right) \leq 0.8L_w \quad (14)$$

A parametric study was presented to determine the length of the plastic hinge of circular RC columns using a three-dimensional finite element analysis [6]. They proposed simplified formulas of plastic hinge length for circular reinforced concrete columns (equations 15 and 16).

$$\frac{L_p}{h} = 0.936\left(\frac{P}{P_o}\right) + 7.398\left(\frac{A_s}{A_g}\right) + 0.06\left(\frac{L}{h}\right) - 0.003(f'_c) \quad \text{For } 414 \text{ MPa} \quad (15)$$

$$\frac{L_p}{h} = 0.503\left(\frac{P}{P_o}\right) + 3.218\left(\frac{A_s}{A_g}\right) + 0.053\left(\frac{L}{h}\right) - 0.0018(f'_c) \quad \text{For } 685 \text{ MPa} \quad (16)$$

Moreover, a parametric study was conducted to derive an analytical model for estimating the length of the plastic hinge of cantilever RC structural walls by using the comprehensive nonlinear finite-element analyses results of [7]. According to the parametric investigation, a plastic hinge length equation was proposed reliant on wall length, axial load ratio, shear span to wall-length ratio and wall horizontal web reinforcement ratio (equation 17).

$$L_p = 0.27L_w \left(1 - \frac{P}{A_w f'_c}\right) \left(1 - \frac{f_y \rho_{sh}}{f'_c}\right) \left(\frac{M/V}{L_w}\right)^{0.45} \quad (17)$$

For these reasons, a finite element analysis was conducted using ABAQUS software on several models to investigate the parameters that have a significant effect on plastic deformation in plastic zone. Also, this analysis was to obtain an equation for the plastic hinge length of slender walls. Before doing these models, a calibration model of a cantilever shear wall [2] was considered to generate key parameters in the model and to analyze depending on experimental test results for a specified specimen that is taken from previous tests. Then experimental results were used to validate the computational models.

2 Finite Element Analysis

A concrete reinforced shear wall was modelled using the finite element method. ABAQUS (v6.14) was chosen to carry out this study. Half-scale experiment results [2] that were available from previous research were used as a reference and compared with the ABAQUS analysis results.

Finite element model of a cantilever shear wall was developed and set as the initial control for the investigation purpose of this project. The work by (Dazio et al., 2009) [2] was used as the reference for comparison with the result from the finite element analysis. Therefore, all the parameters and conditions in the laboratory test were used in the modelling process.

2.1 Control Specimen

The size and the dimensional details of the cantilever RC shear wall have been used according to the lab experiment conducted by (Dazio et al., 2009) [2] as shown in **Figure 1**. It consists of two main parts, the first part which was a cantilever shear wall of 5.55m height, 2m width and 0.15 m thickness. It has at the top of it a portion that was thicker than the thickness of other its parts. The details of reinforcements were comprised of (34 longitudinal bars, 22 rebars with \emptyset 8 diameter and 12 rebars \emptyset 12 diameters) and (horizontal rebars with two straight bars \emptyset 6 @ 150 mm and U shape bars \emptyset 6 @ 150 mm). Some properties are shown in Tables 1 and 2.

Table 1. Summary of the test unit properties [2].

Test unit	Sectional forces at the base				Reinforcement ratios				Stabilizing reinforcement	
	N (kN)	$N/A_g f'_c (-)$	$V/0.8l_w b_w (MPa)$	$\alpha_N = 0.45l_w N/M (-)$	$\rho_{bound} (%)$	$\rho_{web} (%)$	$\rho_{tot} (%)$	$\rho_h (%)$	S(mm)	s/D _{nom} (-)
WSH4	695±6	0.057	1.85	0.31	1.54	0.54	0.82	0.25	No ties	

Table 2. Concrete mechanical properties [2].

Test unit	$\rho_c (kg/m^3)$	$f_{cw} (MPa)$	$f'_c (MPa)$	$E_c (GPa)$
WSH4	2378 ± 15	58.8 ± 1.7	40.9 ± 1.8	38.5 ± 2.0

The second part is the beam foundation that was supporting the upper shear wall. It consisted of a beam fixed boundary condition with 2.8m height, 0.7m width and 0.6 m height. The details of reinforcements are comprised of (8 rectangular shaped bars \emptyset 18 diameters and U shaped 28 rebars with \emptyset 12 diameters).

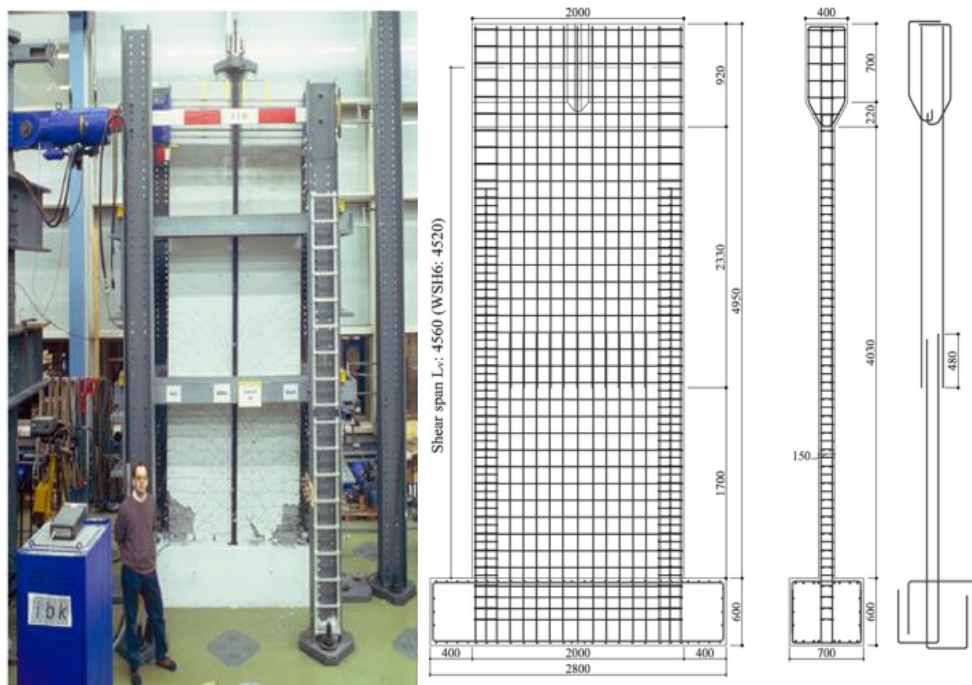


Fig. 1. Experimental Framework and Specimen Dimensions (Dazio et al., 2009) [2].

2.2 Structural Modelling in ABAQUS

Nine models were modelled according to the control specimen to validate FEA results with reference test results as shown below in **Figure 2**.

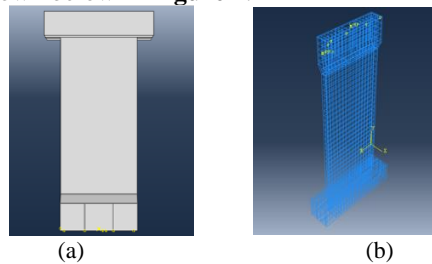


Fig. 2. ABAQUS Model (a) Shear wall module; (b) Shear wall reinforcement.

2.2.1 Creation of Parametric Models

New finite element models of RC shear wall were created with different parameters which they are three models with varying thickness to wall height ratio (t_w/H_w) 0.02 for ($t=10$ cm), 0.024 for ($t=12$ cm) and 0.028 for ($t=14$ cm), other dimensions and properties assumed to be same for the three models which labeled as a model (M1) with the thickness to wall height ratio of (0.02), model (M2) with the thickness to wall height ratio (t_w/H_w) (0.024), and model (M3) with the thickness to wall height ratio (t_w/H_w) (0.028). Besides, three models with varying wall length

($L_w=1.75\text{m}$), ($L_w =1.5 \text{ m}$), and ($L_w=1.25 \text{ m}$), other dimensions and properties will remain the same. These three models labeled as Model 4 (M4) with wall length (L_w) ($L_w=1.75 \text{ m}$), model 5 (M5) with wall length (L_w) ($L_w=1.5 \text{ m}$), and model 6 (M6) with wall length (L_w) ($L_w=1.25 \text{ m}$). Moreover, three models with varying axial load ratio 0.075 for ($P= 925 \text{ kN}$), 0.1 for ($P= 1230 \text{ kN}$), and 0.2 for ($P= 1840 \text{ kN}$), other dimensions and properties will remain the same. These three models labeled as model 7 (M7) with axial load ratio 0.075, model 8 (M8) with axial load ratio 0.1, and model 9 (M9) with axial load ratio 0.15.

2.2.2 Material Models

The properties of the materials were used to be the same for the real model in the experimental test. The Mander's [10] was chosen as the analytical model to simulate the behavior of concrete. This constitutive model was based on the Popovics equation [11]. The concrete damaged plasticity model is based on the plasticity model supposed by Lubliner et al., 1989 [12] and Lee et al., 1998 [13].

2.2.3 Loads

Based on the experimental test [2] an axial load of 695000 N that was applied on the top surface of the model assigned to be constant throughout the analysis process. Besides, a quasi-static monotonic load has been applied on the model (**Figure 9a**). Moreover, a monotonic load was applied in order to establish many results relevant to curvature and rotation as shown in **Figure 9b**. A nonlinear analysis was adopted to predict the components of yield and ultimate curvature under monotonic and axial loads.

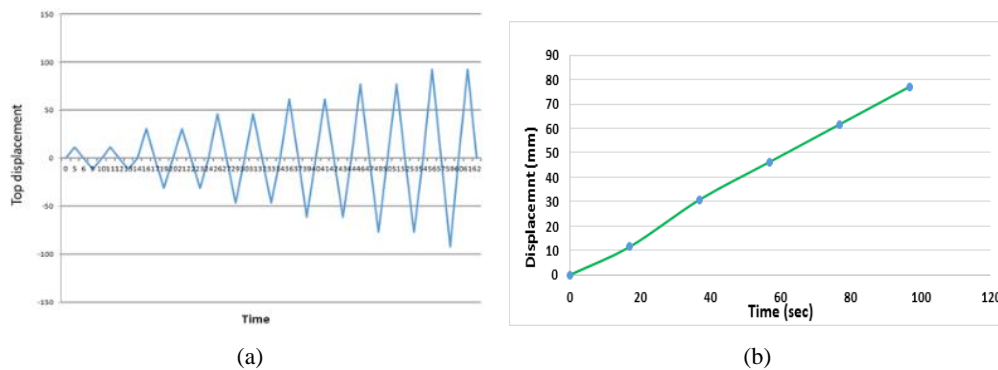


Figure 3. Applied load (a) Load History [2]; and (b) Monotonic Loading.

3. Determination of Plastic Hinge Length (L_p)

Plastic hinge length was determined according to equation (8). When steel and concrete strains for each element in the same row were obtained, the ultimate curvature was calculated according to Kazaz, 2013 [7] as follows. The maximum lateral force that applied to the RC shear wall was corresponding to a maximum drift of ($\delta=1.36 \%$) as stated in Dazio et al., 2009 [2].

3.1 Derivation of Plastic Hinge Length Equation

The multiple regression techniques were adopted in deriving the expression by SPSS statistics software. There were 9 results of parametric models and 3 results of reference mode that were equal 12 results as stated in Table 3. Plastic hinge length calculated as a function of the following parameters: slenderness ratio (t_w/H_w), axial load ratio ($\frac{P}{A_w f_c}$) and wall-length (L_w).

Table 3. The parameters input as independent variables into SPSS software.

$(\frac{P}{A_w f_c})$	(t_w/H_w)	$(L_w)(mm)$
0.058	0.03	2000
0.075	0.03	2000
0.1	0.03	2000
0.15	0.03	2000
0.058	0.03	2000
0.058	0.02	2000
0.058	0.024	2000
0.058	0.028	2000
0.058	0.03	2000
0.058	0.03	1750
0.058	0.03	1500
0.058	0.03	1250

3.1.1 Validation of proposed plastic hinge length expression

The proposed expression was verified with the previous plastic hinge length equations derived numerically by checking its correlation to others individually. The significant properties and a summary of primary experimental results are presented in Table 4.

Table 4. Differences between experimental and FE results.

Ave. of Finite Element Results		Ave. of Experimental Results		Ave. displacement difference		Ave. force difference	
Force (Kn)	Disp.(mm)	Force (Kn)	Disp.(mm)		%		%
0	0	0	0		0		0
379.27	11.28	308.787	11.27		0.062		18.58
403.5	30.52	421.6	30.89		1.2		4.5
375.225	45.725	429.775	46.37		1.39		14.53
364.42	60.23	426.5	61.7		2.38		17.03
366.13	77	331.2	77.1		0.13		9.54

4. Results of the Parametric Study

4.1 Loads vs Displacements

According to **Figure 4a** for M1, M2 and M3 when the axial load ratio increased, the capacity of the maximum load was significantly increased at the same horizontal displacements and maximum drift ratios reduced. It could be seen in **Figure 4b** for M4, M5 and M6 when thickness

to wall length ratios (t_w/H_w) were slightly increased, the ultimate load capacities were also increased, thus these increments led to an increase in the drift ratio for the models. As obvious from **Figure 4c** the resistant load was not highly dropped after it was reached yielding displacement as compared with M1, M2 and M3. This indicates that the thickness to wall-length ratio parameter has a good effect on optimizing the load capacity which was not highly sensitive to very small changes of this parameter. It can be seen in **Figure 4c** that when the wall lengths were decreased, the load and moment capacity has reduced. Moreover, it can be noted that the difference between these curves was highly big because of the inherent correlation between moment capacities and wall lengths therefore load capacities increase by increasing wall lengths.

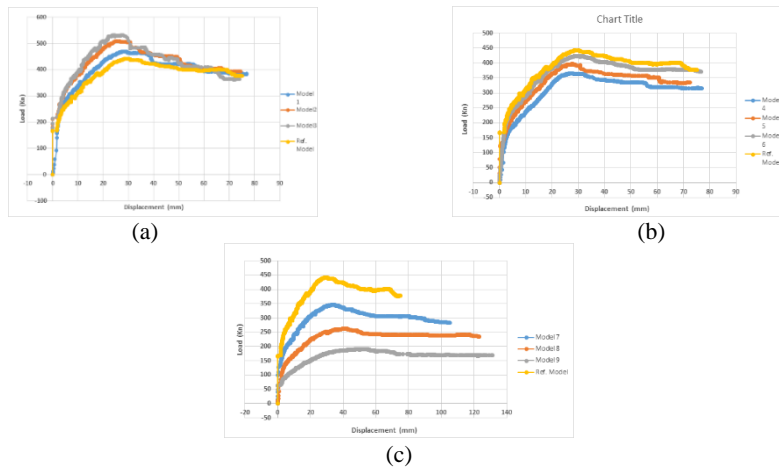


Fig. 4. Load vs Displacement results for (a) Models (1), (2) and (3); (b) Models (4), (5) and (6); and (c) Models (7), (8) and (9).

4.2 Moment - Curvature Curves for Parametric Models

The moment – Curvature curve has stated that the base section curvatures for models (1), (2) and (3) were considerably decreased when the load ratio increased (**Figure 5a**). Drift ratios at which base section curvatures were calculated for these models were δ (1.16%, 1.04% and 0.865%) respectively. These drift ratios also decreased the tensile strains of reinforcing bars in the tension zone of models and thus the total base section curvatures had been reduced. As shown in **Figure 5b**, base section curvatures for models (4), (5) and (6) have been slightly changed when thickness to wall length ratios was small varied because of the little effect of this parameter on-base curvatures. Drift ratios at which base curvatures were determined for these models were δ (1.18%, 1.24% and 1.33%). According to **Figure 5c** reducing wall lengths for models (7), (8) and (9) has led to an increase in the base section curvatures. Thus, drift ratios at which base curvatures were determined for these models considerably increased and they were δ (1.88%, 2.4% and 2.66%). Therefore, the wall-length parameter had a significant effect in increasing base curvatures and drift ratios.

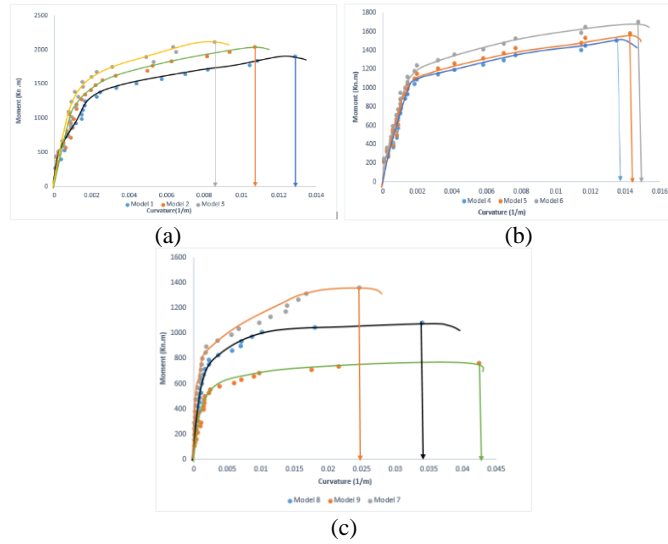


Fig. 5. Moment – Curvature Curve for (a) models (1), (2) and (3); (b) models (4), (5) and (6); and (c) models (7), (8) and (9).

4.3 Plastic Hinge Lengths for Parametric Models

As explained in section 3, the plastic hinge lengths could be done in two ways. The best fit line shown in **Figures 6** and **7** considered more accurately than the direct way by applying equation 8.

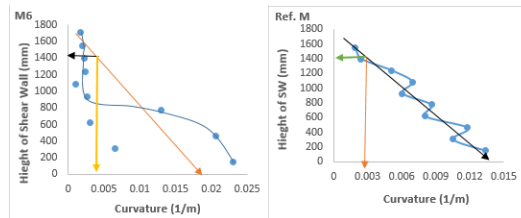


Fig. 6. Calculation of plastic hinge zone for reference and model (6).

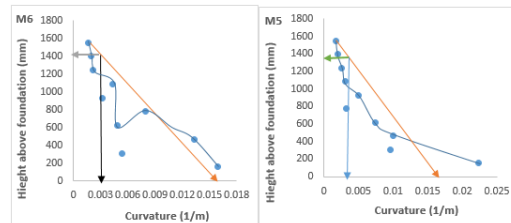


Fig. 7. Calculation of plastic hinge zone for the model (4) and model (5).

According to plastic hinge length results presented in Table 5, it can be noted that most of the parameters that have a significant effect on the plastic hinge length are the model's wall length. On the other hand, the thickness wall height ratio is the most parameter that has a considerable

impact on the results of plastic hinge length especially when the wall thickness is more than 10mm.

Table 5. Plastic hinge length results and the corresponding parameters.

Symbol of model	$L_p(mm)$	R_{AL}	R_{Ht}	$L_w(mm)$
MR	724	0.058	0.03	2000
M1	701	0.075	0.03	2000
M2	682	0.1	0.03	2000
M3	638	0.15	0.03	2000
M4	681	0.058	0.02	2000
M5	698	0.058	0.024	2000
M6	716	0.058	0.028	2000
M7	656	0.058	0.03	1750
M8	606	0.058	0.03	1500
M9	552	0.058	0.03	1250

As shown in **Figure 8a** plastic hinge lengths for reference (1), (2) and (3) have increased as the parameter of axial load ratios decreased. In the contrary, lengths of plastic hinge decreased as base section curvature increased as stated in **Figure 8b**. Moreover, plastic hinge lengths for reference (4), (5) and (6) had increased when the parameter of the wall length increased as shown in **Figure 9**.

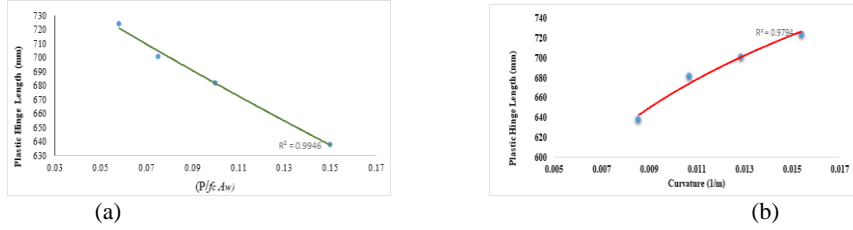


Fig. 8. Plastic Hinge Length for reference, (1), (2) and (3) models (a) Plastic Hinge Length Vs Axial Load Ratio parameter; and (b) Plastic Hinge Length Vs Curvatures of axial load ratio parameter.

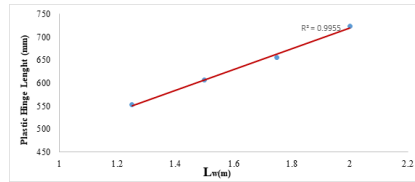


Fig. 9. Plastic Hinge Length vs Wall Length parameter for reference, (7), (8) and (9) models.

5. Derived Plastic Hinge Length Equation

According to the results, it found that the relationship between both axial load ratio, wall-length parameters and the plastic zone length was linear whereas the relation between the thickness to wall height ratio was nonlinear. Based on these findings, the analytical equation was derived as shown in equation (18).

$$L_p = (0.293 L_w) \left(1 - 1.38 \frac{P}{f_c A_w} \right) * \left(\frac{1}{0.033 * (R_{ht}/L_w)^{-0.28}} \right) \quad (18)$$

As seen in **Figure 10a**, the proposed expression derived in this study has good agreement with FE analysis results. As shown in the output file of SPSS software, the R squared related to the accuracy of the derived equation was 92.6%. It can be concluded that the terms of the proposed equation were linear except for the third term that was nonlinear. The plastic hinge length prediction using the derived equation (18) and available from other studies also was compared with finite element analysis results in **Figures 10b, 11, and 12**. These results showed that the best predictions and correlations were obtained by equation (18) proposed in this work.

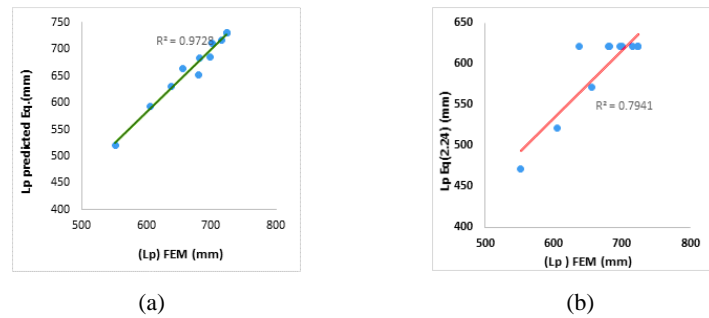


Fig. 10. Comparison of plastic hinge length calculate from FE analysis with predicted equation proposed in (a) this study, Eq. (18); (b) Eurocode 8 [13].

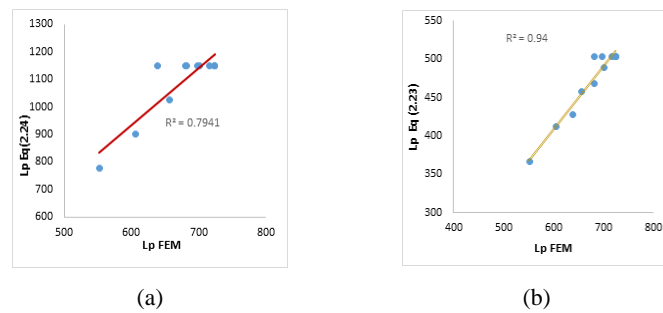


Fig. 11. Comparison of plastic hinge length calculate from FE analysis with (a) Priestley et al. (1996) [14]; (b) According to [15].

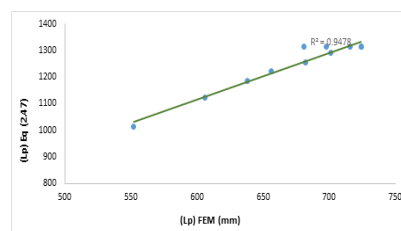


Fig. 12. Comparison of plastic hinge lengths calculated from finite-element analysis with the Bohl and Adebar (2011) [5].

5.1 Verification of proposed expression using experimental data

In order to validate the accuracy of the (L_p) expression that derived analytically, a database comprised of shear wall test results were compiled. The data consisted of 23 small to large scale

shear wall experiments were conducted under static cyclic or monotonic loading for either increasing or variable displacement amplitude. The significant properties and a summary of test results are presented in Table 6. The calculated plastic hinge lengths from the predicted equation (18) are tabulated in the last column in Table 6 as the plastic zone lengths via multiplying them by 2. A comparison between the experimental and calculated L_{pz} values is shown in **Figure 13**. It was noted when compared between the two last columns of Table 6 and **Figure 13**, that there was a clear difference between measured and predicted values. That happened because the predicted results of the plastic zone length were calculated only based on three parameters as explained previously. Experimental values of the plastic zone length determined on the basis of many variables presented in the other columns contributed significantly to the calculation of L_{pz} . These were the reasons that made high standard deviation, a little covariance and a weak correlation between the experimental and predicted values.

Table 6. Test parameters and calculated deformations at yield and ultimate displacement for the wall specimens [7].

No.	specimen	L_w (cm)	t_w (cm)	H_w (cm)	ρ_b %	ρ_{sv} %	ρ_{sh} %	R_{at} %	f'_c Mpa	$\frac{V_{max}}{A_w \sqrt{f'_c}}$	DR %	L_{pz} (exp.)	L_{pz} Pred.
1	PCA-R1	191	10.2	457	1.47	0.25	0.31	0.4	44.7	0.09	2.26	1.83	1.403
2	PCA-R2	191	10.2	457	4	0.25	0.31	0.4	46.4	0.16	2.92	2.06	1.403
3	PCA-B1	191	10.2	457	1.11	0.29	0.31	0.3	53	0.19	2.89	2.06	1.403
4	PCA-B2	191	10.2	457	3.67	0.29	0.63	0.3	53.6	0.49	2.27	1.83	1.403
5	PCA-B3	191	10.2	457	1.11	0.29	0.31	0.3	47.3	0.21	3.93	2.13	1.403
6	PCA-B4	191	10.2	457	1.11	0.29	0.31	0.3	45	0.25	5.94	2.74	1.403
7	PCA-B5	191	10.2	457	3.67	0.29	0.63	0.3	45.3	0.58	2.77	1.83	1.403
8	PCA-B6	191	10.2	457	3.67	0.29	0.63	14.1	21.8	0.9	1.71	1.52	1.136
9	PCA-B7	191	10.2	457	3.67	0.29	0.63	7.9	49.3	0.71	2.89	2.29	1.26
10	PCA-B8	191	10.2	457	3.67	0.29	1.38	9.3	42	0.77	2.86	2.29	1.23
11	PCA-B9	191	10.2	457	3.67	0.29	0.63	8.9	44.1	0.75	3.02	2.29	1.24
12	PCA-B10	191	10.2	457	1.97	0.29	0.63	8.6	45.6	0.53	2.77	2.13	1.243
13	PCA-F1	191	10.2	457	3.89	0.3	0.71	0.4	38.5	0.69	1.11	1.83	1.402
14	UCB-SW3	239	10.2	309	3.52	0.83	0.83	7.8	34.8	0.76	5.67	2	1.65
15	UCB-SW4	239	10.2	309	3.52	0.83	0.83	7.5	35.9	0.69	2.25	2	1.66
16	UCB-SW5	241	10.2	309	6.34	0.63	0.63	7.3	33.4	0.64	2.24	1.8	1.673
17	UCB-SW6	241	10.2	309	6.34	0.63	0.63	7	34.5	0.6	2.33	1.4	1.68
18	UCB-RW2	122	10.2	382	2.89	0.33	0.33	7	43.7	0.25	2.19	0.9	0.97
19	WS2	200	15	452	1.32	0.3	0.25	5.7	40.5	0.19	1.39	1.4	1.5
20	WS3	200	15	452	1.54	0.54	0.25	5.8	39.2	0.24	2.04	1.7	1.5
21	WS4	200	15	452	0.67	0.27	0.25	12.8	38.3	0.24	1.37	1.4	1.34
22	WS6	200	15	452	1.54	0.54	0.25	10.8	45.6	0.29	2.07	1.6	1.386
23	WI	163	12.7	1133	0.66	0.45	0.45	10	35	0.11	2	1.9	0.9

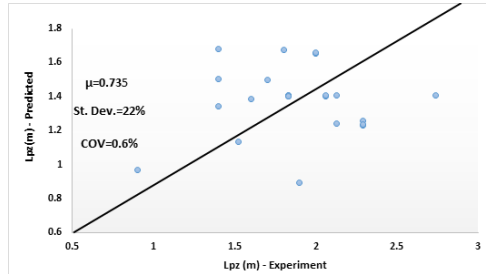


Fig. 13. Comparison of plastic zone lengths between measured and predicted.

6. Conclusion

This study showed that the comparison of the FE analysis results to the experimental results displayed good agreement in the load-displacement envelope curve and maximum forces. On the other hand, the moment and load the capacity of RC shear wall models have been significantly increased as axial load ratios were increased. Besides, bearing capacities have been improved when thickness to wall height ratios was increased. Moreover, the lateral strength capacity of RC shear wall models has been dropped when the wall-length parameter was reduced. Furthermore, base section curvatures were decreased as axial load ratios and the wall-length increased. It found that good agreement and correlation obtained for the predicted plastic hinge equation when compared with other numerically derived expressions. Then, the proposed equation was verified with data available from experimental studies.

References

- [1] Moehle, J. P.: Displacement-Based Design of RC Structures Subjected to Earthquakes. *Earthquake Spectra*, 8(3), 403 – 428 (1992)
- [2] Dazio, A., Beyer, K., & Bachmann, H.: Quasi-static cyclic tests and plastic hinge analysis of RC structural walls. *Engineering Structures*, 31(7), 1556-1571 (2009)
- [3] (CEN), E. C. for S.: Eurocode 8: Design of structures for earthquake resistance: Part 3: Assessment and retrofitting of buildings. BS EN 1998-3, Brussels, Belgium (Vol. 1) (2005)
- [4] Panagiotakos, T.B., and Fardis, M. N.: Deformations of Reinforced Concrete Members at Yielding and Ultimate.” *ACI Structural Journal*, 98(2), 135 – 148 (2001)
- [5] Bohl, A., and Adebar, P.: Plastic hinge lengths in high-rise concrete shear walls. *ACI Struct. J.*, 108(2), 148–157 (2011)
- [6] Ou, Chen, Raditya Andy, N.: Plastic hinge length of reinforced concrete columns. *ACI Structural Journal*, 105(3), 290–300 (2012)
- [7] Kazaz, I.: Analytical Study on Plastic Hinge Length of Structural Walls, (November), 1938–1950 (2013)
- [8] Mun, J.: Plastic hinge length of reinforced concrete slender shear walls, 67(8) (2014)
- Oesterle, R.G., Aristizabal-Ochoa, J.D., Shiu K.N., and Corley, W. G. (1984). “Web Crushing of Reinforced Concrete Structural Walls.” *ACI Journal*, 81(3), 231 – 241.
- [9] Mander, J. B., Priestley, M. J. N., and R. Park.: Theoretical Stress Strain Model for Confined Concrete. *Journal of Structural Engineering* (1988)
- [10] Popovics.: A numerical approach to the complete stress-strain curve of concrete. *Cement and Concrete Research*, 3(5) (1973)
- [11] LUBLINER, Oller, & Barcelona, C.: A plastic-damage model for concrete. *International Journal of Solids and Structures*, 25(3), 299–326 (1989)
- [12] Lee, J. and Fenves, G.: Plastic-Damage Model for Cyclic Loading of Concrete Structures. *Journal of Engineering Mechanics*, 124(8), 892–900 (1998)
- [13] (CEN), E. C. for S.: Eurocode 8: Design of structures for earthquake resistance: Part 3: Assessment and retrofitting of buildings. BS EN 1998-3, Brussels, Belgium (Vol. 1), (2005)
- [14] Priestley, M. J. N., Seible, F., and Calvi, G. M.: *Seismic design and retrofit of bridges*. Wiley, New York, (1996)
- [15] Paulay, T., and Priestley, M. J. N.: *Seismic design of reinforced concrete and masonry buildings*. Isbn-10 (Vol. 471549150) (1992)